

## On Smooth Feynman Propagators for Real Time Path Integrals

Nancy Makri

School of Chemical Sciences, University of Illinois, 505 S. Mathews Avenue, Urbana, Illinois 61801

Received: October 14, 1992; In Final Form: December 3, 1992

In this paper we consider various ways of obtaining Feynman propagators that lack the standard highly oscillatory coordinate dependence and discuss their usefulness for Monte Carlo evaluation of the real time path integral. Using truncated basis set expansions to construct appropriate projection operators, we propose simple schemes for incorporating important potential features in the smoothing of a propagator. We point out that the object to be examined in order to determine the efficiency of a particular smoothing scheme is not the shape of the effective propagator itself but rather the product of two such propagators; thus, propagators that appear less oscillatory are not necessarily better behaved. Finally, we discuss the performance of Monte Carlo methods in real time path integral calculations with effective propagators.

### 1. Introduction

The possibility of using the path integral formulation of quantum mechanics<sup>1</sup> to perform exact quantum dynamical calculations on many-particle systems has intrigued theoretical chemists for many years. The idea is to express the propagator for an arbitrary time  $t$  in terms of short-time propagators, for which simple approximations are available. Thus, in the case of a time-independent  $F$ -dimensional Cartesian Hamiltonian

$$\hat{H} = \sum_{i=1}^F \frac{\hat{p}_i^2}{2m} + V(\hat{x}_1, \dots, \hat{x}_F) \equiv \hat{T} + \hat{V} \quad (1.1)$$

the coordinate representation of the propagator takes the form<sup>1,2</sup>

$$\langle \mathbf{x} | e^{-i\hat{H}t/\hbar} | \mathbf{x}_0 \rangle = \int d^F \mathbf{x}_1 \dots \int d^F \mathbf{x}_{N-1} \prod_{k=1}^N \langle \mathbf{x}_k | e^{-i\hat{H}\Delta t/\hbar} | \mathbf{x}_{k-1} \rangle \quad (1.2)$$

where  $\mathbf{x}_N \equiv \mathbf{x}_f$ . For sufficiently small  $\Delta t$ , the short-time propagators that appear in the integrand of the above equation are often approximated by the Trotter formula:<sup>2</sup>

$$\langle \mathbf{x}_k | e^{-i\hat{H}\Delta t/\hbar} | \mathbf{x}_{k-1} \rangle = \left( \frac{m}{2\pi i \hbar \Delta t} \right)^{F/2} \exp \left( \frac{i}{\hbar} \left[ \frac{m}{2\Delta t} |\mathbf{x}_k - \mathbf{x}_{k-1}|^2 - \Delta t V(\mathbf{x}_k) \right] \right) \quad (1.3)$$

Because in its conventional formulation the path integral is a multidimensional integral, Monte Carlo techniques<sup>3</sup> provide the only possible way to evaluate it numerically. Importance sampling methods have proven extremely useful for simulating equilibrium (i.e., imaginary time) properties of many-particle systems. In contrast, the case of real time dynamics appears to be substantially more difficult to deal with, due to the oscillatory nature of the time-evolution operator. In recent years, significant effort has been expended toward developing numerical techniques for evaluating path integrals in real time.<sup>4-18</sup>

A major step toward this goal was the development of stationary phase based Monte Carlo methods,<sup>8-10,12-14</sup> which take advantage of the semiclassical limit of the path integral.<sup>2</sup> The integrand is modified to incorporate an exponential factor involving the derivative of the action along the discretized path, and thus highly oscillatory contributions that arise from nonclassical paths are damped. These methods are very efficient for sampling around a single classical path (and thus for obtaining short to intermediate time dynamics in most ordinary cases) but converge very slowly if the dynamics is dominated by many interfering classical trajectories.

A different approach was introduced in 1989<sup>11,12</sup> and recently pursued further by other groups.<sup>15,16</sup> The idea is to construct an *effective* system-specific propagator, which is sufficiently accurate for the particular problem but which results in a less oscillatory integrand than the standard short-time propagator; one can then attempt direct Monte Carlo evaluation of the path integral using these effective propagators. Here we define an effective propagator as a function  $K_{\text{eff}}(\mathbf{x}_0, \mathbf{x}_f, \Delta t)$  which satisfies the relation

$$\Psi(\mathbf{x}_f, t + \Delta t) = \int d^F \mathbf{x}_0 K_{\text{eff}}(\mathbf{x}_0, \mathbf{x}_f, \Delta t) \Psi(\mathbf{x}_0, t) + \Delta \Psi \quad (1.4)$$

where  $\Delta \Psi$  is an error that arises from replacing the exact propagator by  $K_{\text{eff}}$  and which can be made arbitrarily small by adjusting the parameters that enter in the definition of the effective propagator. Clearly, an effective propagator must satisfy at least two requirements in order to be useful: it must yield a *smooth* integrand as a function of the path integral coordinates, and it must die off outside a certain range.

The extent of smoothing that can be performed on the propagator depends on the particular application under consideration. Note that in order to describe correctly quantum mechanical effects the effective propagator has to be a complex function and thus the integrand in the discretized path integral expression will be at least somewhat oscillatory. Given the enormous difficulty that Monte Carlo integration methods face when the integrand alternates in sign, it is apparent that the potential of path integral calculations with effective propagators will not be unlimited. Nevertheless, it is likely that some interesting problems can be dealt with successfully by using these ideas.

The first scheme for constructing smooth effective propagators, which I proposed in 1989, consisted in using a truncated basis set of plane wave functions to project out large momentum components that are responsible for the highly oscillatory behavior of the short time propagator.<sup>11</sup> In a recent series of subsequent papers,<sup>16</sup> Hoffman *et al.* used a set of Hermite fitting functions to construct a different approximate smooth propagator. Both of these approaches dealt only with the *kinetic* energy part of the Hamiltonian and resulted in translationally invariant propagators that decay with the separation of the coordinate points. As a consequence, the paths sampled according to those schemes consist of random free-particle steps, with the probability of a given step decreasing with length. Since the only constraint imposed on these paths is of kinematic nature, the majority of them explore regions of space with very large *potential* energy, which are *insignificant* to the dynamics. Such paths interfere destructively with one another due to phase factors that arise from the potential terms in the propagator and thus make no contribution to the

result in principle, but this dramatic phase cancellation generally causes the Monte Carlo statistics to be poor.

It is obvious from the above discussion that a successful smoothing of the propagator must take into account the potential—at least in a crude fashion—such that the paths selected by Monte Carlo according to the particular sampling distribution will not be allowed to explore physically unimportant regions. In this paper we show that simple expressions for such propagators can indeed be constructed with truncated basis set projection procedures.

A different formulation of the path integral, in terms of propagators constructed numerically on a grid, has been discussed in other recent papers by our group.<sup>17,18</sup> That approach leads to a powerful fully quantum mechanical method for extracting the dynamics in the special case of a system coupled to a harmonic bath. The efficiency of that method has been demonstrated by our converged calculations on intramolecular energy flow in a six-degree-of-freedom system over five vibrational periods<sup>18</sup> and by our propagation of wave functions through potential barriers in a ten-degree-of-freedom symmetric double-well potential.<sup>17</sup> The question of whether our numerically constructed propagators will be of practical utility in more general cases is currently under investigation by our group. In any case, these procedures for constructing improved propagators numerically are not likely to be applicable to problems with highly complex potential interactions. Thus, throughout this paper we restrict consideration to smooth propagators that can be obtained in terms of functions known analytically, which are applicable in cases where numerical propagators may not be easy to obtain.

In section 2 we use the truncated basis set idea<sup>11</sup> to construct propagators that are designed to sample only the dynamically relevant regions, thus minimizing phase cancellation problems. We derive a spatially confined propagator that is exponentially damped outside the region of space explored by the wave function. For those degrees of freedom in a multidimensional problem that are only moderately anharmonic, we construct a smooth harmonic reference propagator that is accurate over longer time steps and that helps reduce potential phase oscillations even further.

The performance of these propagators in Monte Carlo calculations is discussed in section 3. We point out that the efficiency of a particular smoothing procedure is not determined simply by the shape of the effective propagator itself but rather by the decay characteristics of the product of two such propagators. As a consequence, propagators that appear less oscillatory are not necessarily better behaved. We compare these and previous propagators in light of this observation and discuss general issues related to Monte Carlo statistics in real time path integral calculations. Finally, section 4 concludes.

## 2. Smooth Spatially Confined Propagators

In order to keep the notation simple, we consider a one-dimensional Hamiltonian of the form

$$\hat{H} = \frac{\hat{p}^2}{2m} + V(\hat{x}) \equiv \hat{T} + \hat{V} \quad (2.1)$$

The multidimensional generalization of the propagators that will be discussed in this paper is straightforward.

The most common procedure of approximating the propagator for short time  $\Delta t$  is based on the symmetrized Trotter splitting<sup>2</sup> of the time-evolution operator,

$$\exp(-i\hat{H}\Delta t/\hbar) \approx \exp(-i\hat{V}\Delta t/2\hbar) \exp(-i\hat{T}\Delta t/\hbar) \times \exp(-i\hat{V}\Delta t/2\hbar) \quad (2.2)$$

Use of this approximation leads to the following coordinate

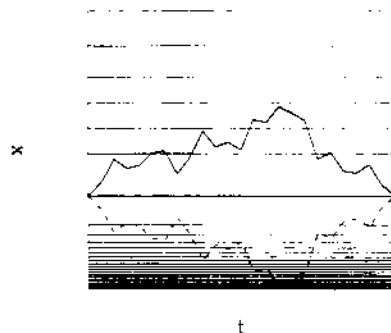


Figure 1. Schematic representation of two discretized paths as a function of time. Solid line: path A. Dashed line: path B, penetrating steep potential regions. The horizontal lines represent Morse potential contours. The shaded area indicates high potential regions of no relevance to the dynamics.

propagator, valid for short time:

$$\langle x_f | e^{-i\hat{H}\Delta t/\hbar} | x_0 \rangle \approx \langle x_f | e^{-i\hat{T}\Delta t/\hbar} | x_0 \rangle e^{-i(\Delta t/2\hbar)[V(x_f) + V(x_0)]} \quad (2.3)$$

If the free particle part is evaluated exactly, one obtains the standard result

$$\langle x_f | e^{-i\hat{T}\Delta t/\hbar} | x_0 \rangle = \left( \frac{m}{2\pi i \hbar \Delta t} \right)^{1/2} \exp \left[ \frac{i}{\hbar} \frac{m}{2\Delta t} (x_f - x_0)^2 \right] \quad (2.4)$$

The last expression is a highly oscillatory function of the coordinates. These rapid oscillations in eq 2.4, along with the fact that the modulus of this propagator does not decay with increasing distance, prohibit use of Monte Carlo methods in the evaluation of the path integral.

Previous smoothing schemes used finite sets of translationally invariant functions to project out highly oscillatory components<sup>11,12,15</sup> or produce an approximate fit<sup>16</sup> of the propagator. Both methods resulted in effective propagators that lack the rapid oscillations of eq 2.4 and whose magnitude decreases with distance. Due to these properties, these propagators can indeed be used for direct Monte Carlo evaluation of the path integral.

However, both previous effective propagators are by construction translationally invariant, i.e., their modulus decays with the separation of the coordinate points. This constrains the total length of the paths chosen by a Monte Carlo procedure but involves no bias of a dynamical nature. As the Monte Carlo weight for these paths does not depend on potential parameters, a large number of Monte Carlo moves will be wasted in regions where the potential energy is high; such paths correspond to rapidly oscillatory phase factors and thus make the convergence of a path integral extremely slow. The situation is illustrated in Figure 1, which considers propagation of a wave function in a Morse potential. Shown is a typical path starting and ending at the potential minimum (path A), composed of small discrete steps, such that the above translationally invariant short-time propagators have significant magnitude. Also shown is the mirror image of path A (path B), which consists of steps of lengths equal to those in path A. Because such propagators have a modulus that decays with the separation of the coordinate points, paths A and B enter the path integral with identical weights. I.e., a Monte Carlo calculation with translationally invariant propagators will spend just as much time sampling paths like B as it will spend sampling near path A. Path B, however, is seen to penetrate the steep repulsive part of the potential quite deeply, and therefore the phase factors associated with the potential part will vary extremely rapidly with small variations of the path. It is precisely these phase factors that statistical sampling methods cannot deal with.

We mention parenthetically that these rapid phase variations do not occur if the path integral is evaluated by matrix multiplication (which of course is only possible for low-dimensional systems): the coordinate range  $[x_{\min}, x_{\max}]$  and therefore all paths

are restricted in these methods, and unphysical regions of steeply rising potential are not accessible.

It is clear from the above discussion that in order to perform efficient Monte Carlo sampling, one would like to impose a *dynamical constraint* on the paths selected that prevents them from entering regions of very high potential energy. In the example of Figure 1, one would like the sampling procedure to exclude paths similar to B but integrate thoroughly over paths such as A. A brute-force algorithm that accomplishes this would be to examine for each path selected all the coordinates, rejecting the path if *any one* of the coordinates lies outside the predetermined physically important range. Mathematically, this procedure would be equivalent to multiplying each short-time propagator by a square window function:

$$K_{\text{eff}}(x_{k-1}, x_k; \Delta t) \rightarrow K_{\text{eff}}(x_{k-1}, x_k; \Delta t) \theta\left(\frac{x_k - x_{\min}}{x_{\max} - x_{\min}}\right) \quad (2.5)$$

where  $\theta(x) = 1$  for  $0 < x < 1$  and zero otherwise. (Inclusion of a similar factor for  $x_{k-1}$  is superfluous, since that point coincides with the "final" point for the next short-time propagator in the path integral.) This procedure would be the Monte Carlo generalization of grid propagation methods. However, we suspect that such abrupt cutoff of the weighting function will lead to poor Monte Carlo sampling. In part a we propose an alternate (but just as simple) way of restricting the range of each short-time propagator *smoothly*, by making its modulus decay as *each* of the end points, independently, becomes large. In part b we specialize to problems where the Hamiltonian (for some or all degrees of freedom) can be expanded about a harmonic reference and show how the potential can be taken into account in the smoothing procedure.

Following our previous approach,<sup>11</sup> we use again truncated basis sets to project out high-energy components of the kinetic energy propagator. The fact that any well-behaved wave function  $\Psi$  has a finite expansion (in the sense that the expansion coefficients  $c_n$  drop off exponentially with  $n$  for  $n$  larger than a certain  $n_{\max}$ ) in a basis set that spans the same Hilbert space leads to effective completeness relations (finite energy projection operators) of the type

$$\hat{1} = \sum_{n=0}^{n_{\max}} |\Phi_n\rangle \langle \Phi_n| + O(\epsilon) \quad (2.6)$$

where  $\epsilon = \langle \Phi_{n_{\max}} | \Psi \rangle$ .

In ref 11 an effective kinetic energy propagator was obtained by projecting on plane waves of momentum smaller than a cutoff  $p_{\max}$ . These functions provide the natural basis for expanding the kinetic energy propagator, as the latter is *diagonal* in the momentum representation. In order to construct a propagator with the above desirable properties, though, we must use basis functions that are not translationally invariant. Rather, we must choose basis functions that can describe well the region of space explored by the wave function during its evolution but that decay to zero outside this region. The basis functions must be chosen according to standard considerations; i.e., they must span the range of interest, such that the propagated wave function can be expressed in terms of these basis functions at any instant in time (within the time scale of interest).

**(a) Expansion in Truncated Harmonic Oscillator Basis.** The first smoothing scheme that we propose here is based on the Trotter partitioning of the time-evolution operator, eq 2.2. We use a truncated basis set of harmonic oscillator (THO) eigenstates  $\{\Phi_n\}$  to construct an effective completeness relation valid in that specific coordinate range. Assuming for notational simplicity that the relevant coordinate range extends from  $-x_{\max}$  to  $x_{\max}$  (i.e., defining the center of the interval that we want to cover as

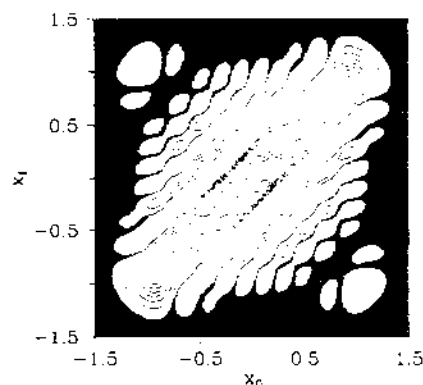


Figure 2. Contour plot of the real part of the THO propagator as a function of the end points  $x_0$  and  $x_f$ .

$x = 0$ ), we expand the propagator as follows:

$$\langle x_f | e^{-i\hat{T}\Delta t/\hbar} | x_0 \rangle_{\text{THO}} \equiv \sum_{n=0}^{n_{\max}} \langle x_f | e^{-i\hat{T}\Delta t/2\hbar} | \Phi_n \rangle \langle \Phi_n | e^{-i\hat{T}\Delta t/2\hbar} | x_0 \rangle \quad (2.7a)$$

where

$$\Phi_n(x) = \frac{\alpha^{1/4}}{\pi^{1/4}} (2^n n!)^{-1/2} H_n(\alpha^{1/2} x) e^{-(\alpha/2)x^2} \quad (2.7b)$$

are harmonic oscillator eigenfunctions with spatial extent on the order of  $\pm x_{\max}$ .

Because of the use of harmonic oscillator basis functions in eq 2.7a, the kinetic energy operator is not diagonal here. Inserting a complete set of momentum eigenstates, we write

$$\begin{aligned} \langle x | e^{-i\hat{T}\Delta t/2\hbar} | \Phi_n \rangle &= \int_{-\infty}^{\infty} dp \langle x | e^{-i\hat{T}\Delta t/2\hbar} | p \rangle \langle p | \Phi_n \rangle \\ &= (2\pi\hbar)^{-1/2} \frac{\gamma^{1/4}}{\pi^{1/4}} (2^n n!)^{-1/2} i^n \times \\ &\quad \int_{-\infty}^{\infty} dp \exp\left[-\frac{\gamma}{2} + \frac{i\Delta t}{4\hbar m} p^2 + \frac{i}{\hbar} xp\right] H_n(\gamma^{1/2} p) \end{aligned} \quad (2.8)$$

where  $\gamma = 1/\hbar^2\alpha$ . Performing the Gaussian integral leads to the result

$$\begin{aligned} \langle x | e^{-i\hat{T}\Delta t/2\hbar} | \Phi_n \rangle &= \frac{\alpha^{1/4}}{\pi^{1/4}} (2^n n!)^{-1/2} \frac{\sigma(0)}{\sigma(\Delta t/2)} \left( \frac{\sigma^*(\Delta t/2)}{\sigma(\Delta t/2)} \right)^n \times \\ &\quad \exp\left[-x^2/2\sigma^2(\Delta t/2)\right] H_n\left(\alpha^{1/2} \frac{|\sigma(0)|^2}{|\sigma(\Delta t/2)|^2} x\right) \end{aligned} \quad (2.9a)$$

with

$$\sigma^2(0) = 1/\alpha \quad \text{and} \quad \sigma^2(\Delta t) = \sigma^2(0) + i\hbar\Delta t/m \quad (2.9b)$$

We thus obtain the following expression for the effective propagator:

$$\begin{aligned} \langle x_f | e^{-i\hat{T}\Delta t/2\hbar} | x_0 \rangle_{\text{THO}} &= \frac{\alpha^{1/4}}{\pi^{1/4}} \eta(\Delta t) \exp[-(x_0^2 + x_f^2)/ \\ &\quad 2\sigma^2(\Delta t/2)] \sum_{n=0}^{n_{\max}} \frac{i}{2^n n!} \left( \frac{\sigma^*(\Delta t/2)}{\sigma(\Delta t/2)} \right)^{2n} H_n(-\alpha^{1/2} |\eta(\Delta t)| x_0) \times \\ &\quad H_n(\alpha^{1/2} |\eta(\Delta t)| x_f) \end{aligned} \quad (2.10)$$

where

$$\eta(t) \equiv \sigma(0)^2 / \sigma(\Delta t/2)^2$$

Equation 2.10 contains an exponential damping factor that depends on each of the coordinate points *separately*, and thus the propagator decays to zero when either  $x_0$  or  $x_f$  becomes large. This asymptotic behavior is seen very clearly in Figure 2, which

shows a contour plot of the real part of this propagator. However, this figure also shows that for values of  $x_0$  and  $x_f$  smaller than  $x_{\max}$  the magnitude of the propagator actually decays with the coordinate separation  $|x_f - x_0|$ . This is accomplished by the Hermite terms in eq 2.10. Therefore, the THO propagator behaves similarly to the previous translationally invariant propagators when the end points are well inside the physically relevant region of space, and thus short paths will enter with larger weight; on the other hand, the asymptotic dominance of the exponential factor guarantees that the weight of a path goes to zero very rapidly if that particular path attempts to wander outside the preselected physically important region of space. Large potential regions, which would cause extremely rapidly oscillatory behavior, are thus avoided this way.

**(b) Effective Harmonic Reference Propagator.** Previous work on closed-form propagators, and also this paper so far, has restricted attention to propagators derived from the Trotter splitting of the time-evolution operator, eq 2.2. The various smoothing schemes dealt with the kinetic energy part, which is responsible for the violent oscillations that the real-time propagator exhibits at small  $\Delta t$ . As we argued at the beginning of this section though, smoothing the kinetic energy factor alone is not adequate because purely kinematic constraints cannot prevent multiple-step paths from entering steep potential regions, where the potential part of the propagator becomes highly oscillatory. In part of this section we proposed a way of incorporating minimal dynamical information in the smoothed kinetic energy propagator by making it exponentially small outside the region of configuration space visited by the wave function. Here we show how the remaining oscillations due to the potential can be reduced further by incorporating *the entire quadratic part* of the Hamiltonian in the smoothed effective propagator. The idea is similar to the harmonic reference propagator of Friesner and Levy<sup>19</sup> and is expected to offer an improved numerical scheme in cases where the harmonic approximation provides a reasonable zeroth-order reference. Some other cases where the best reference Hamiltonian is separable or adiabatic but very anharmonic can be dealt with according to our numerically constructed propagators on a grid.<sup>17,18</sup>

In order to proceed, we write

$$\hat{H} = \hat{H}_0 + \hat{V}_{\text{anharmonic}} \quad (2.11a)$$

where

$$\hat{H}_0 = \hat{T} + (1/2)m\omega^2\hat{x}^2 \quad (2.11b)$$

is the harmonic reference Hamiltonian that incorporates the best quadratic fit to the potential, and  $\hat{V}_{\text{anharmonic}}$  contains the remaining anharmonic potential terms. (Again we assumed without loss of generality that the origin has been shifted to coincide with the potential minimum.) Use of a symmetric splitting of the time evolution operator leads to the following effective harmonic reference (EHR) coordinate propagator:

$$\langle x_f | e^{-i\hat{H}\Delta t/\hbar} | x_0 \rangle_{\text{EHR}} \approx e^{-iV_{\text{anharmonic}}(x_f)\Delta t/2\hbar} \times \langle x_f | e^{-i\hat{H}_0\Delta t/\hbar} | x_0 \rangle_{\text{EHR}} e^{-iV_{\text{anharmonic}}(x_0)\Delta t/2\hbar} \quad (2.12)$$

Equation 2.12 is the real-time analog of the splitting suggested by Friesner and Levy for equilibrium problems.<sup>19</sup> The part involving the quadratic reference  $\hat{H}_0$  is the propagator for a harmonic oscillator and therefore is known analytically. However, the *exact* harmonic oscillator propagator is highly oscillatory and thus not suitable for the present purpose. Instead of substituting the analytic expression for the harmonic reference propagator,<sup>19</sup> we expand it in a truncated basis set in order to filter out the oscillatory high-energy contributions. The obvious basis set is in this case that of the eigenstates  $\Phi_n$  of  $\hat{H}_0$  already

used above to smooth out the kinetic energy part:

$$\langle x_f | e^{-i\hat{H}_0\Delta t/\hbar} | x_0 \rangle_{\text{EHR}} = \sum_{n=0}^{n_{\max}} \Phi_n(x_f) \Phi_n(x_0) e^{-i[n+(1/2)]\omega\Delta t} \quad (2.13)$$

where  $\omega$  is the harmonic frequency, defined by eq 2.11b. In the limit where  $n_{\max}$  approaches infinity, eq 2.13 approaches the exact propagator for a harmonic oscillator.

To implement the above scheme in multidimensional problems, one needs to identify a suitable harmonic reference. Normal mode type coordinates, in which the quadratic reference Hamiltonian is separable (and the effective propagator factorizable), will often be well suited.

As in the case of the THO propagator, the use of harmonic oscillator functions causes the modulus of the EHR propagator to be exponentially damped if either of the two end points penetrates regions inaccessible to the wave packet. However, rather than serving merely as a high-energy filter, the basis functions are in the present case eigenstates of the closely related harmonic reference problem and thus contain true dynamical information. Furthermore, the important new feature of the EHR propagator is that the oscillatory factor that arises from the potential term is now better behaved. Specifically, it is clear from eq 2.12 that the complex exponential factors will now cause rapid oscillations only if the *anharmonicity* (and not the potential itself) is large. This is not the case with effective propagators based on the Trotter splitting; the latter contain phase factors that oscillate violently in regions where the potential rises rapidly—even if it does so in a quadratic fashion.

Thus, use of the EHR propagator guarantees that the integrand of the path integral will be smooth (and therefore suitable for Monte Carlo methods) if the potential is not too strongly anharmonic. On the other hand, many important problems involve potentials for which no adequate global harmonic reference exists. However, a common situation in problems with many degrees of freedom is that all but one or two of the coordinates are nearly harmonic (but not truly harmonic and thus cannot be integrated out explicitly by using influence functionals). Use of EHR propagators for those degrees of freedom will prevent highly oscillatory phase factors from appearing in these mildly anharmonic coordinates and will therefore enhance the efficiency of such calculations.

Another important advantage offered by the above splitting of the propagator is that eq 2.12 is valid for time much longer than eq 2.3, which uses the kinetic energy term as the reference Hamiltonian. (In fact, this was the main idea in ref 19.) This means that the EHR propagator can be used with larger time steps in the path integral, and thus fewer integration variables will be required for a given total time  $t$ . As will become apparent in the next section, the improvement in the Monte Carlo statistics as the number of integration variables decreases is dramatic in cases where the integrand is oscillatory, and thus the present scheme should improve the convergence of real-time path integral calculations even further.

### 3. Features and Monte Carlo Statistics

In this section we analyze the characteristics of the various effective propagators that have been suggested and discuss their performance in Monte Carlo path integral calculations.

**(a) Comparison of Various Effective Propagators.** The spatially confined propagators presented in section 2 incorporate the dynamical information necessary for Monte Carlo integration methods to avoid unphysical potential regions. Clearly, an additional requirement in order for these techniques to be useful is that the propagators must yield a smooth integrand when used in the path integral, so that minimal phase cancellation takes place.

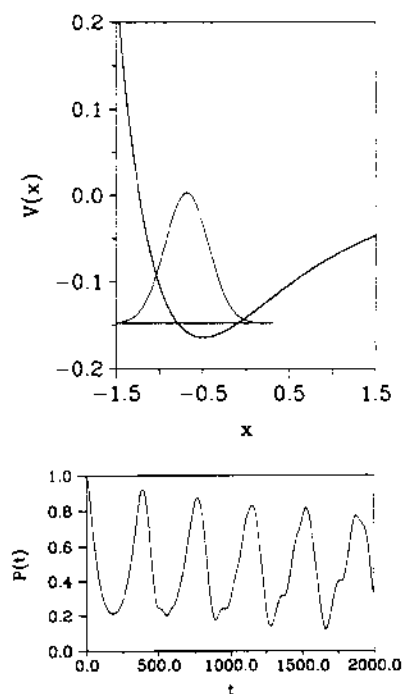


Figure 3. The model problem considered for the illustration throughout this paper. The values of the parameters are given in the Appendix. (a, Top) The Morse potential and the initial state. (b, Bottom) The survival probability (calculated by exact propagation) over about five vibrational periods. All units are atomic units.

We first compare the various kinetic energy propagators. In order to present an objective comparison, we have chosen the parameters of these propagators such that an initially displaced Gaussian is propagated correctly in a Morse potential over at least five vibrational periods (see Figure 3). The details are given in the Appendix. Needless to say, the one-dimensional Morse potential serves here only as a model for assessing the advantages and limitations of these techniques for use in truly multidimensional problems.

Figure 4 shows the real and imaginary parts of the THO propagator of section 2a and compares with the two previous translationally invariant propagators, the TPW propagator<sup>11</sup> and the DAF propagator.<sup>16</sup> The truncated plane wave (TPW) propagator was constructed<sup>11</sup> with a basis of plane waves as the high-energy (momentum) filter:

$$\langle x_f | e^{-i\hat{T}\Delta t/\hbar} | x_0 \rangle_{\text{TPW}} \equiv \int_{-p_{\text{max}}}^{p_{\text{max}}} dp \langle x_f | e^{-i\hat{T}\Delta t/2\hbar} | p \rangle \langle p | e^{-i\hat{T}\Delta t/2\hbar} | x_0 \rangle = \left( \frac{m}{2\pi i \hbar \Delta t} \right)^{1/2} e^{(i/\hbar)(m/2\Delta t)(x_f - x_0)^2} f_{\text{smooth}}(x_f - x_0; p_{\text{max}}; \Delta t) \quad (3.1a)$$

where the function  $f_{\text{smooth}}$  is given by

$$f_{\text{smooth}}(x_f - x_0; p_{\text{max}}; \Delta t) = \frac{1}{2} \operatorname{erf} \left( \left( \frac{i\Delta t}{2m\hbar} \right)^{1/2} p_{\text{max}} + \left( \frac{im}{2\hbar\Delta t} \right)^{1/2} (x_f - x_0) \right) + \frac{1}{2} \operatorname{erf} \left( \left( \frac{i\Delta t}{2m\hbar} \right)^{1/2} p_{\text{max}} - \left( \frac{im}{2\hbar\Delta t} \right)^{1/2} (x_f - x_0) \right) \quad (3.1b)$$

Here  $\operatorname{erf}(z)$  is the error function of complex argument,<sup>20</sup>

$$\operatorname{erf}(z) = \frac{2}{\pi^{1/2}} \int_0^z e^{-x^2} dx$$

and  $p_{\text{max}}$  is a cutoff value of momentum chosen according to the

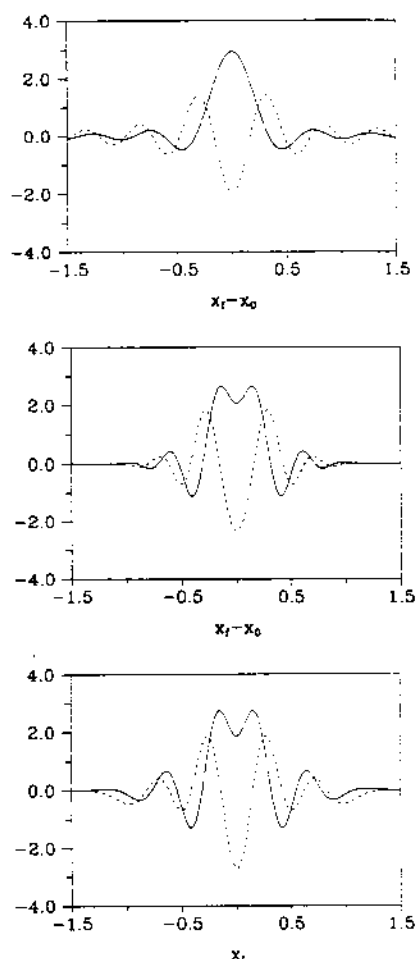


Figure 4. (a, Top) The TPW propagator with  $p_{\text{max}} = 13$  as a function of the difference  $x_f - x_0$  of the end points. (b, Middle) The DAF propagator with  $\sigma = 0.23$  and  $n_{\text{max}} = 7$  as a function of the difference  $x_f - x_0$  of the end points. (c, Bottom) the THO propagator with  $\alpha = 16.27$  and  $n_{\text{max}} = 9$  as a function of  $x_f$  with  $x_0 = 0$ . The time increment is 20 atomic units in all three cases. Solid line: real part. Dashed line: imaginary part.

accuracy desired. The error due to the above momentum truncation is of order  $\Psi(p_{\text{max}})$ , where  $\Psi(p)$  is the wave function in momentum space. Since wave functions typically decay exponentially with momentum, it is easy to choose a cutoff value  $p_{\text{max}}$  to make the error as small as desired.

For finite values of the momentum cutoff  $p_{\text{max}}$ ,  $f_{\text{smooth}}$  acts as a smoothing and damping factor in the short-time propagator. I.e., for short time and large separation of the coordinate points, such that no classical particle starting at  $x_0$  with momentum smaller than  $p_{\text{max}}$  can reach  $x_f$  in time  $\Delta t$ , it can be shown<sup>11</sup> that

$$f_{\text{smooth}}(x_f - x_0; p_{\text{max}}; \Delta t) \propto \frac{1}{x_f - x_0} e^{-(i/\hbar)(m/2\Delta t)(x_f - x_0)^2} \times \sin[p_{\text{max}}(x_f - x_0)/\hbar] \quad (3.1c)$$

The exponential factor of the above equation cancels the rapid oscillations of the kinetic energy propagator,<sup>11,12</sup> resulting in a smooth propagator that decays as  $|x_f - x_0|^{-1}$ .

The distributed approximating function (DAF) propagator was obtained<sup>16</sup> by fitting the full free-particle propagator with propagated translationally invariant Hermite functions  $f_n(x_f - x_0)$ , where

$$f_n(x) = e^{-(\alpha/2)x^2} H_n \left( \frac{\alpha^{1/2}}{2^{1/2}} x \right) \quad (3.2)$$

leading to the following result:

$$\langle x_j | e^{-i\hat{T}\Delta t/\hbar} | x_0 \rangle_{\text{DAF}} = \frac{1}{\sigma(\Delta t)} e^{-(x_j - x_0)^2 / 2\sigma^2(\Delta t)} \sum_{n=0}^{n_{\text{max}}} \left(-\frac{1}{4}\right)^n \times \left(\frac{\sigma(0)}{\sigma(\Delta t)}\right)^{2n+1} \frac{1}{(2\pi)^{1/2} n!} H_{2n}((x_j - x_0) / 2^{1/2} \sigma(\Delta t)) \quad (3.3)$$

with  $\sigma$  given by eq 2.9b. Because the above fitting procedure does not correspond to a rigorous quantum mechanical principle, the DAF propagator is not strictly unitary. Since, however, real-time Monte Carlo path integral calculations are typically characterized by fairly sizable error, the lack of unitarity of the DAF propagator may not be of practical significance.

The use of Gaussian functions in the DAF and THO propagators is reflected in their asymptotic behavior. In contrast, the use of Fourier basis functions makes the TPW propagator decay as  $|x_j - x_0|^{-1}$ . This "slow" decrease with distance in the magnitude of the TPW propagator has been criticized in recent papers by Hoffman et al.<sup>16</sup> By examining the real part of this propagator, these authors conclude that the TPW propagator is too oscillatory and long-ranged to allow successful evaluation of the path integral by Monte Carlo techniques. In fact, examination of the *imaginary* part of the TPW propagator reveals that the size of the negative lobes is on the same order as the size of the positive ones. This is also the case with the two exponentially damped propagators and appears to imply that Monte Carlo sampling with any of these effective propagators will be extremely poor. The situation is altered drastically, however, if one realizes that *each variable appears twice in the integrand of the path integral*, cf. eq 1.2; i.e., the relevant quantity to examine (with any effective propagator  $K_{\text{eff}}$ ) is not the propagator itself, but the product

$$K_{\text{eff}}(x_{k-1}, x_k; \Delta t) K_{\text{eff}}(x_k, x_{k+1}; \Delta t) \quad (3.4)$$

Figure 5 shows the real and imaginary parts of this product as a function of the path integral variable  $x_k$  at fixed values of  $x_{k-1}$  and  $x_{k+1}$  for the same three kinetic energy propagators. In contrast to the behavior of the bare propagators, it is seen that this critical product is *best behaved* (i.e., most localized and smooth) in the case of the TPW propagator. Yet, the THO propagator offers the advantage of confining paths inside the physically important region of space, which is important in multiple-step path integral calculations.

Finally, in order to compare the efficiency of the EHR propagator in Monte Carlo path integral calculations with that of effective propagators based on the Trotter splitting, we must consider the question of optimal time step. This point is discussed below in conjunction with the statistics of Monte Carlo algorithms.

**(b) Monte Carlo Statistics.** It is important to emphasize that the construction of improved effective propagators can substantially enhance the convergence of real time path integral calculations (and thus allow more interesting problems to be dealt with) but will not entirely eliminate the "sign problem". Unlike ordinary cases of positive integrands, where the required number of Monte Carlo points increases slowly with dimension, Monte Carlo evaluation of the real time path integral with effective propagators requires effort that grows *exponentially* with the number of time discretizations  $N$ . This is so because the volume in multidimensional space corresponding to negative values of the integrand becomes comparable to the volume of positive regions very rapidly as  $N$  is increased.

To make this last point more transparent, consider the integrand in the path integral calculation of the survival amplitude for a

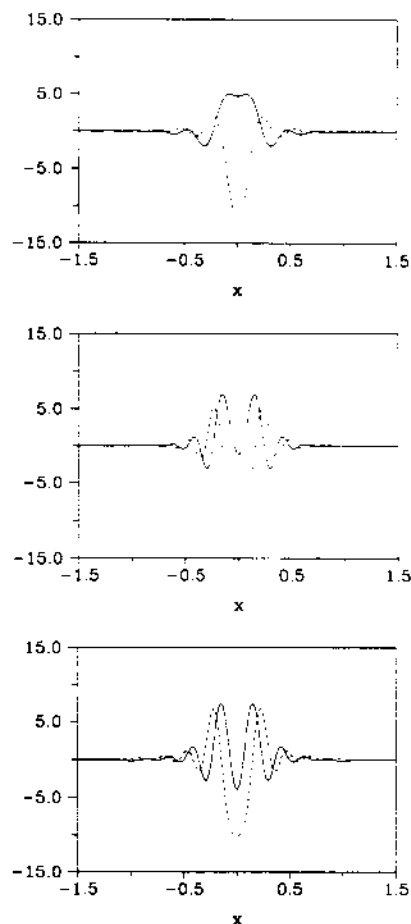


Figure 5. The product  $\langle x_j | e^{-i\hat{T}\Delta t/\hbar} | x \rangle_{\text{eff}} \langle x | e^{-i\hat{T}\Delta t/\hbar} | x_0 \rangle_{\text{eff}}$  as a function of  $x$  for  $x_1 = x_2 = 0$  for the three effective kinetic energy propagators shown in Figure 4. (a, top) TPW propagator; (b, middle) DAF propagator; (c, bottom) THO propagator.

state which at  $t = 0$  is a Gaussian wave packet (and thus positive everywhere):

$$S(t) = \int dx_0 \int dx_1 \dots \int dx_N \langle \Psi(0) | x_N \rangle \times K_{\text{eff}}(x_{N-1}, x_N; \Delta t) \dots K_{\text{eff}}(x_0, x_1; \Delta t) \langle x_0 | \Psi(0) \rangle \quad (3.5)$$

where  $\Delta t = t/N$ . In order to get an estimate of the work required to evaluate the above integral by Monte Carlo, we have calculated separately the integrals of the positive and negative areas of the real and imaginary parts of the integrand in eq 3.5 as a function of  $N$ . The difference between positive and negative integrals is the desired survival amplitude. Clearly, the Monte Carlo statistics will be good only if the result (i.e., the above difference) is significantly larger than the statistical error in the calculation of the positive and negative integrals separately. Figure 6 shows the difference between positive and negative integrals, relative to the sum of these two quantities,

$$R_N = \frac{|\text{integral of positive} - |\text{integral of negative}||}{\text{integral of positive} + |\text{integral of negative}|} \quad (3.6)$$

for the real and imaginary parts of eq 3.5 with one of the effective kinetic energy propagators as a function of  $N$  with fixed time step  $\Delta t$ . (All effective propagators show qualitatively similar scaling behavior, so we present a single figure.) We will refer to this quantity as the *cancellation index*. For simplicity we have not included potential phase factors in the calculation of  $R_N$ ; potential phases introduce additional oscillations, and we discussed ways of dealing with them efficiently in section 2. The maximum of  $R_N$  at  $N = 2$ , which indicates best Monte Carlo statistics for this

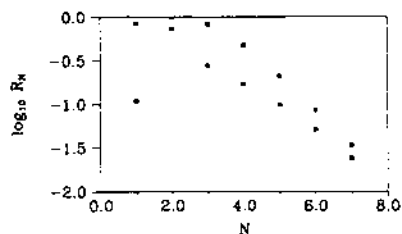


Figure 6. Cancellation index, eq 3.6, as a function of the number of time slices  $N$  calculated with one of the effective kinetic energy propagators with time step  $\Delta t = 20$  au. Solid squares: real part. Open squares: imaginary part.

value of  $N$ , is consistent with the observation in section 2 that the product of two propagators is better behaved than a single propagator. It is clear from Figure 6 that the above quantity decreases geometrically (i.e., exponentially) with the number of time slices if a fixed time step is used. Although the fractional statistical error in the individual Monte Carlo evaluation of the positive and of the negative integral can be made fairly small, it is clear that by increasing  $N$  (and thus the total time  $t$ ) one will eventually reach a value  $N_{\text{critical}}$  beyond which  $R_N$  is smaller than the fractional Monte Carlo error attainable with a given amount of numerical effort. In order to maintain statistical error smaller than the result of the calculation for  $N > N_{\text{critical}}$ , one must increase the total number of Monte Carlo points. Since  $R_N$  decreases exponentially with  $N$ , it is apparent that the required Monte Carlo effort grows exponentially with  $N$  (and thus with the total time  $t$ ). The critical value of  $N$  above which the quantity  $R_N$  drops below the achievable fractional statistical uncertainty will of course depend on the parameters of the problem and on the smoothness of the effective propagator used; however, it is clear that, if one tries to exceed this critical number of integration variables in the real time path integral, the calculation will very soon become unmanageable. This behavior is qualitatively different from that observed in imaginary time Monte Carlo path integral calculations, where the integrand is positive.

Another question that arises in the real time path integral concerns the optimal choice of time step. Generally, effective short-time propagators become more oscillatory as  $\Delta t$  is increased. However, the more pronounced oscillatory behavior that results by increasing the time increment is more than counterbalanced by the reduction in the number of integration variables required for propagation to a given time  $t$ . To see this, consider a short-time propagator of time step  $\Delta t$  vs a product of two propagators of step  $\Delta t/2$  in the path integral:

$$K_{\text{eff}}(x_{k-1}, x_k; \Delta t) \approx \int dx' K_{\text{eff}}(x', x_k; \Delta t/2) K_{\text{eff}}(x_{k-1}, x'; \Delta t/2) \quad (3.7)$$

[Equation 3.7 would be an identity if exact rather than effective propagators were used.] Even though the shorter time propagators in the last equation will generally be better behaved than the one with time increment  $\Delta t$ , the oscillations in the path integral as functions of  $x_k$  and  $x_{k-1}$  are clearly identical in both sides of eq 3.7. However, the right-hand side of that equation, where the propagator is expressed in terms of two propagators of length  $\Delta t/2$ , has the disadvantage of requiring one additional numerical integration by Monte Carlo.

The gain achieved by using larger time steps is illustrated in Figure 7, which shows the cancellation index  $R_N$  as a function of  $N$  for fixed total time  $t$ . It is clear that the largest step propagator will perform best. We therefore conclude that it is advantageous from the point of view of Monte Carlo statistics to use as large a time step as allowed by the particular splitting of the time evolution operator. For this reason also, in addition to the dynamical sampling considerations discussed in section 2, the EHR propagator will be better behaved than effective Trotter propagators whenever a reasonable harmonic reference exists.

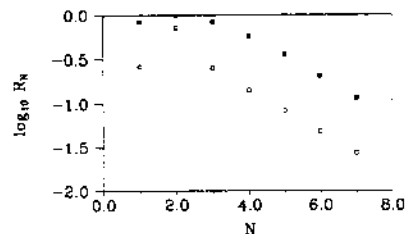


Figure 7. Cancellation index, eq 3.6, as a function of the number of time slices  $N$  calculated with one of the effective kinetic energy propagators for total time  $t = 50$  au.

#### 4. Concluding Remarks

We have discussed and compared various schemes for constructing effective short-time propagators that lack the standard highly oscillatory coordinate dependence. We pointed out that the actual performance of an effective propagator in the path integral is not governed by the precise shape of the bare propagator but rather by the behavior of the product of two such propagators. This is an obvious point with somewhat unexpected consequences. Specifically, use of the propagator product as the efficiency criterion of various propagators leads to the conclusion that the TPW propagator<sup>11</sup> whose real and imaginary parts fall off relatively slowly results in an integrand that is less oscillatory compared to the integrand obtained with exponentially damped propagators.

We also argued that use of translationally invariant functions in the smoothing of the propagator leads to inefficient Monte Carlo sampling governed by pure kinematic considerations. In order to exclude paths of large potential energy (which correspond to rapidly oscillatory phase factors), the absolute value of the propagator must include at least minimal dynamical information. In section 2 we described a simple scheme that accomplishes this within the Trotter splitting of the time-evolution operator, as well as an improved procedure that takes into account the quadratic part of the potential. The latter scheme will minimize phase oscillations and allow larger time steps in problems with nearly harmonic degrees of freedom, while the former is applicable to more general situations. Finally, Hamiltonians with a well-characterized (e.g., separable, adiabatic, etc.) anharmonic zeroth-order reference are still best dealt with by using our numerically constructed propagators on a grid,<sup>17,18</sup> since these are accurate for fairly long time and yield sampling functions that reflect the special characteristics of the particular problem.

In conclusion, it appears that effective smooth propagators can be of considerable utility in certain problems, since they allow numerical evaluation of the real time path integral with fairly simple Monte Carlo sampling schemes. The ability of these techniques to deal with long-time dynamics is clearly limited and will depend strongly on the validity of the propagator over large time increments. In this regard, improved splittings of the time evolution operator, whenever practical, can dramatically enhance the convergence of long time path integral calculations.

**Acknowledgment.** This work has been supported in part by the Petroleum Research Fund, administered by the American Chemical Society.

#### Appendix

In order to illustrate the behavior and to allow an objective comparison of the effective propagators discussed in this paper, we consider propagation of a wavepacket in a Morse potential that characterizes the vibration of the  $H_2$  molecule. The potential in our model is

$$V(x) = D(e^{-2\beta x} - 2e^{-\beta x}) \quad (A.1)$$

with  $D = 0.164$  and  $\beta = 0.9374$  atomic units. The mass is equal

to the reduced mass of H<sub>2</sub>, i.e.,  $m = 918.5$  au. The initial state is a Gaussian displaced by  $-0.1$  Å from equilibrium, with width equal to that of the lowest eigenstate of the harmonic approximation at the minimum (see Figure 1A). The survival probability,

$$P(t) = |\langle \Psi(t) | \Psi(0) \rangle|^2 \quad (\text{A.2})$$

that corresponds to this initial state is shown in Figure 1B over about five vibrational periods.

The parameters  $p_{\text{max}}$ ,  $n_{\text{max}}$ , and  $\sigma$  that enter in the definition of the various effective propagators are chosen such that the survival probability is reproduced to within approximately 1% over the time shown in Figure 1B. The time step  $\Delta t$  used to plot propagators based on the Trotter splitting of the time evolution operator was chosen equal to 20 atomic units of time (i.e., about 0.5 fs, or  $1/18$  of the vibrational period); significantly larger time steps introduce errors, while use of smaller time steps results in unnecessary increase of the number of integration variables in the path integral (i.e., worse Monte Carlo statistics).

### References and Notes

- (1) Feynman, R. P. *Rev. Mod. Phys.* **1948**, *20*, 367. Feynman, R. P.; Hibbs, A. R. *Quantum Mechanics and Path Integrals*; McGraw-Hill: New York, 1965.
- (2) Schulman, L. S. *Techniques and Applications of Path Integration*; Wiley: New York, 1981.
- (3) Metropolis, N.; Rosenbluth, A. W.; Rosenbluth, M. N.; Teller, H.; Teller, E. *J. Chem. Phys.* **1953**, *21*, 1087. Valleau, J. P.; Whittington, S. G. In *Modern Theoretical Chemistry*; Berne, B. J., Ed.; Plenum: New York, 1977; Vol. 5, pp 137-168.
- (4) Thirumalai, D.; Berne, B. J. *Chem. Phys. Lett.* **1985**, *116*, 471. Thirumalai, D.; Berne, B. J. *Annu. Rev. Phys. Chem.* **1986**, *37*, 401.
- (5) Behrman, E. C.; Jongeward, G. A.; Wolynes, P. G. *J. Chem. Phys.* **1983**, *79*, 6277. Behrman, E. C.; Wolynes, P. G. *J. Chem. Phys.* **1985**, *83*, 5863. Wolynes, P. G. *J. Chem. Phys.* **1987**, *87*, 6559. Cline, R. E., Jr.; Wolynes, P. G. *J. Chem. Phys.* **1988**, *88*, 4334. Mason, B. A.; Hess, K.; Cline, R. E.; Wolynes, P. G. *Superlattices and Microstructures* **1987**, *3*, 421.
- (6) Doll, J. D. *J. Chem. Phys.* **1984**, *81*, 3536. Doll, J. D.; Freeman, D. L. *Science* **1986**, *234*, 1356. Doll, J. D.; Coalson, R. D.; Freeman, D. L. *J. Chem. Phys.* **1987**, *87*, 1641.
- (7) Chang, J.; Miller, W. H. *J. Chem. Phys.* **1987**, *87*, 1648.
- (8) Filinov, V. S. *Nucl. Phys. B* **1986**, *271*, 717.
- (9) Makri, N.; Miller, W. H. *Chem. Phys. Lett.* **1987**, *139*, 10. Makri, N.; Miller, W. H. *J. Chem. Phys.* **1988**, *89*, 2170.
- (10) Doll, J. D.; Freeman, D. L. *Adv. Chem. Phys.* **1988**, *73*, 120. Doll, J. D.; Freeman, D. L.; Gillan, M. J. *Chem. Phys. Lett.* **1988**, *143*, 277. Doll, J. D.; Beck, T. L.; Freeman, D. L. *J. Chem. Phys.* **1988**, *89*, 5753. Beck, T. L.; Doll, J. D.; Freeman, D. L. *J. Chem. Phys.* **1989**, *90*, 3181.
- (11) Makri, N. *Chem. Phys. Lett.* **1989**, *159*, 489.
- (12) Makri, N. *Comp. Phys. Commun.* **1991**, *63*, 389.
- (13) Mak, C.; Chandler, D. *Phys. Rev. A* **1990**, *41*, 5709. Mak, C. H.; Chandler, D. *Phys. Rev. A* **1991**, *44*, 2352.
- (14) Mak, C. *Phys. Rev. Lett.* **1992**, *68*, 899.
- (15) Sharafeddin, O. A.; Kouri, D. J.; Nayar, N.; Hoffman, D. J. *Chem. Phys.* **1991**, *95*, 3224.
- (16) Hoffman, D. K.; Nayar, N.; Sharafeddin, O. A.; Kouri, D. J. *J. Phys. Chem.* **1991**, *95*, 8299. Hoffman, D. K.; Kouri, D. J. *J. Phys. Chem.* **1992**, *96*, 1179. Hoffman, D. K.; Arnold, M.; Kouri, D. J. *J. Phys. Chem.* **1992**, *96*, 6539.
- (17) Makri, N. *Chem. Phys. Lett.* **1992**, *193*, 435. Makri, N. *NATO ASI*, in press.
- (18) Topaler, M.; Makri, N. *J. Chem. Phys.*, in press.
- (19) Friesner, R. A.; Levy, R. M. *J. Chem. Phys.* **1984**, *80*, 4488. Zhang, P.; Levy, R. M.; Friesner, R. A. *Chem. Phys. Lett.* **1988**, *144*, 236.
- (20) Abramowitz, M.; Stegun, I. A. *Handbook of Mathematical Functions*; U.S. Government Printing Office: Washington, DC, 1964.